Mechatronic Systems 2

Applications in Material Handling Processes and Robotics

Edited by
Leonid Polishchuk
Orken Mamyrbayev
Konrad Gromaszek

ROUTLEDGE

Mechatronic Systems 2

Mechatronic Systems 2

Applications in Material Handling Processes and Robotics

Edited by

Leonid Polishchuk
Vinnytsia National Technical University, Vinnytsia, Ukraine

Orken Mamyrbayev
Institute of Information and Computational Technologies CS MES RK, Almaty, Kazakhstan

Konrad Gromaszek
Lublin University of Technology, Lublin, Poland

Routledge
Taylor & Francis Group
LONDON AND NEW YORK

Cover image: Andrzej Kotyra
First published 2021
by Routledge/Balkema
Schipholweg 107C, 2316 XC Leiden, The Netherlands
e-mail: enquiries@taylorandfrancis.com
www.routledge.com – www.taylorandfrancis.com

Routledge/Balkema is an imprint of the Taylor & Francis Group, an informa business

Library of Congress Cataloging-in-Publication Data
A catalog record has been requested for this book

ISBN: 978-1-032-10585-7 (Hbk)
ISBN: 978-1-032-12621-0 (Pbk)
ISBN: 978-1-003-22544-7 (eBook)

DOI: 10.1201/9781003225447

Typeset in Times New Roman
by codeMantra

Contents

Chapter 16

Investigation of interaction of a tool with a part in the process of deforming stretching with ultrasound

N. Weselowska, V. Turych, V. Rutkevych, G. Ogorodnichuk, P. Kisała, B. Yeraliyeva, and G. Yusupova

CONTENTS

16.1 INTRODUCTION

The current development of hydraulic cylinders requires their developers to further improve their technical level, competitiveness and to expand functional capabilities. Requirements for the working surfaces of hydraulic cylinders are increasing – the accuracy of holes in terms of the permissible deviations from axial straightness and non-circularity, the working surface roughness, the surface microrelief, as well as the increase of working pressures. These requirements can be successfully fulfilled by a technological process based on stretching deformation using ultrasound (Kumar 2013, Mashkov et al. 2014, Turych & Rutkevych 2016). In this connection, the task of developing the technology of cylinder sleeves is topical.

16.2 ANALYSIS AND PROBLEM STATEMENT

The problem of improving the accuracy of hollow detail surfaces of machine parts such as sleeves and cylinders is highlighted by many authors, namely Proskuryakov Yu. G., Rosenberg O. A Posvyatenko E. K. (Turych & Rutkevych 2016, Turych et al. 2017). However, from the standpoint of resource conservation, which is extremely important for the Ukrainian economy, these processes are not sufficiently studied. Since the adhesion phenomena in the process of treatment of materials by cold plastic deformation are certainly harmful, a number of process researchers recommend the use of oils with high screening properties, that is, anti-agglutinating materials, in which the fillers are molybdenum disulfide, graphite, and other similar substances, which are able to withstand high contact pressure, provide a reliable separation of the surfaces of parts and tools during processing and low external friction coefficient values (0.07–0.1)

DOI: 10.1201/9781003225447-16

(Kumar 2013). However, this method of dealing with adhesion is unsuitable for cold plastic deformation finishing processes, since it does not allow the possibility of lowering the roughness of the surfaces, obtaining high values of deformation strength, texture, and useful compressive stresses in the surface layer. The problem of increasing the accuracy of surface treatment of machine parts such as hollow-type cylinder liners has been covered by many authors, namely Proskuryakov Y. G., Rosenberg A. A., Posvyatenkom E. K., etc. (Moriwaki 2010, Turych et al. 2017, 2018). However, from the resource standpoint, which is extremely important for the Ukrainian economy, these processes have been insufficiently studied. Since adhesion phenomena in the processing of materials by cold plastic deformation are undoubtedly harmful, some process researchers have recommended the use of oils with high screening properties such as adhesive coatings materials, fillers, including molybdenum disulfide, graphite, and similar substances able to withstand high contact pressure, provide reliable separation of the surfaces of parts and tools during processing and a low external friction coefficient (0.07–0.1) (Romashkyna 2009, Shao-Yi et al. 2016).

Several studies show that during cold plastic deformation using ultrasonic vibrations, i.e., using periodic forced separation of the tool and the parts during processing, the quality is improved greatly and the intensity of operations is reduced, as a result of periodic recess into the surface of the part and immediate termination of contact between surfaces of the tools and parts (Kumar 2013, Titov et al. 2017, Turych et al. 2018, Tymchyk et al. 2018).

The conducted studies are relevant to solve practical problems of using such methods.

16.3 PURPOSE, OBJECTIVES, MATERIALS, AND METHODS

The aim of the study is to improve the processing of hollow machine part surfaces such as sleeves and cylinders by stretching deformation using ultrasound and to define the theoretical dependencies in order to calculate the pulling forces during contact between the tool and the part.

A description of the ultrasonic deforming through stretching with ultrasound has been developed based on the application of rheological models of materials that reflect their actual elastic–plastic properties. Such an approach makes it possible to identify the mechanism of how the ultrasound impacts the process of stretching deformation. A study of force parameters was carried out using a loading chart of a perfect elastic–plastic body. Investigation of the machining method's effect on torque involved the following materials: Steel 10, aluminum alloy AK4.

16.4 RESEARCH RESULTS

The use of stretching deformation operations can reduce processing complexity and increase the hydraulic drive reliability and durability by improving the quality of cylinder holes.

The application of ultrasonic technology allows expanding the technological capabilities of stretching deformation, namely: by increasing the hole precision, axial straightness of the cylinder and opening, creating a microrelief on the inner surface to maintain lubrication (Turych & Rutkevych 2016, Turych et al. 2018).

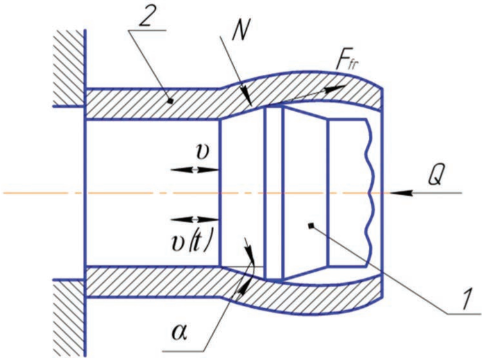

Figure 16.1 Ultrasound stretching schematic.

For the development of the technological process, we consider the contact interaction of the tool with the part during stretching deformation with the use of ultrasound. Figure 16.1 shows a schematic of stretching deformation using ultrasound (Polishchuk et al. 2016, 2018, 2019).

The deforming element 1 oscillates harmonically with an amplitude of ξ and passes through the hole of part 2 with a static force of *Q*. The equation of motion of the deforming element can be represented as follows

$$u(t) = \text{vt} + \xi \sin \omega t \tag{16.1}$$

where v – speed of the tool; t – time; $\omega = 2\pi f$, here f – the frequency of oscillation.

Moving the deforming element leads to a displacement of the contact surfaces of the tool and the part along the normal direction leading to the formation of a working cone tool:

$$u_n(t) = u(t)\sin\alpha \tag{16.2}$$

and to the bias by the tangent:

$$u_\tau(t) = u(t)\cos\alpha \tag{16.3}$$

here α – the inclination angle of the formation of a working cone of the deforming element.

By moving, (16.2) and (16.3) cause normal tension q_n with a resultant N and tangential stresses q_τ with a resultant F_{fr}.

Due to the fact that the tools (16.2), (16.3) are intermittent in nature, the stretching deformation process will take place in three stages, namely: elastic, plastic, and unloading. By analogy with (Rimkeviciene et al. 2009), let's consider the load diagram of ideal elastic–plastic material. The load diagram is shown in Figure 16.2.

The diagram shows: (1) zone of elastic loading; (2) zone of plastic deformation; (3) unloading zone. In view of (16.2), (16.3), the loading characteristics are expressed as follows:

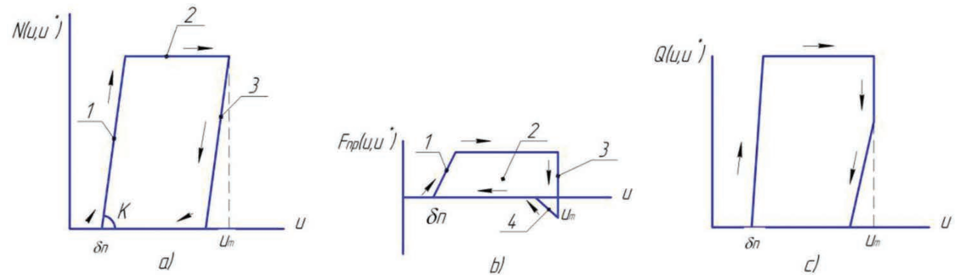

Figure 16.2 The load diagram at $F_{fr} = \eta \cdot N$.

$$N(u_n,\dot{u}_n)=\begin{cases}0 & u_n \le \Delta_n & \dot{u}\ge 0\\ k_n(u_n-\Delta_n)\sin\alpha & \Delta_n \le u_n \le \Delta_n + S & \dot{u}\ge 0\\ N & \Delta_n + S \le u_n \le u_{nm} & \dot{u}\ge 0\\ N-k_n(u_{nm}-u_n)\sin\alpha & u_{nm}-S\le u_n \le u_{nm} & \dot{u}\le 0\\ 0 & u_n \le u_{nm}-S & \dot{u}\le 0\end{cases} \tag{16.4}$$

where k_n – the rigidity of the section of the detail in the normal direction; N – normal force during plastic deformation; Δ – coordinate of the beginning of surface contact of tools and parts; u_{nm} – the maximum mean of the function within a period (16.1); $S = N/k_n \sin\alpha$ – the movement of the deforming element to achieve the normal force of N, that is appropriate for plastic deformation (Kozlov et al. 2019, Ogorodnikov et al. 2018, Ogorodnikov, Dereven'ko, et al. 2018).

Let us consider that between the working surface of the tool and the treated surface during their relative tangential displacement, a friction force occurs directed toward the opposite direction of movement.

$$|F_{fr}| \le \eta N \tag{16.5}$$

A sign of equality (16.5) is placed when slipping occurs. In the absence of slipping the friction force is equal to the classic tangential force. Taking into account the above, it is worth considering the following three cases.

Case I. Friction force $|F_{fr}| = \eta N$

The characteristic of a tangential interaction is as follows:

$$F_{fr}(u,\dot{u}) = \eta \cdot N(u,\dot{u}) sign\dot{u} \tag{16.6}$$

The characteristic of the friction force in the direction of the motion has the following form:

$$F_{frv}(u,\dot{u}) = \eta N(u,\dot{u})\cos\cdot\alpha \cdot sign\dot{u} \tag{16.7}$$

In (16.7) F_{frv} accepts the following values

$$\eta \cdot N(u,\dot{u})\cos\alpha \cdot sign\dot{u} = \begin{cases} \eta \cdot N(u,\dot{u})\cos\alpha & \dot{u} \ge 0 \\ -\eta \cdot N(u,\dot{u})\cos\alpha & \dot{u} \le 0 \end{cases} \tag{16.8}$$

The total characteristic in the direction of movement that is stretching force:

$$Q(u,\dot{u}) = N(u,\dot{u})\sin\alpha + F_{fr}(u,\dot{u})\cos\alpha \tag{16.9}$$

Figure 16.2b shows the dependence (16.8). In Sections 16.1 and 16.2, characteristics of friction force (Figure 16.2b) corresponding to the load result in the sliding of surfaces; in Section 16.3, unloading takes place, followed by elastic negative tension, in Section 16.4 – unloading with slipping. In Figure 16.2c, the solid line shows the total characteristic. The total characteristic describes all possible situations (Figure 16.2c).

The case, as described above, can be considered as a limiting transition since the relative slip of the tool and the part is preceded by a shift of the treated surface together with the tool (Landeta 2015). Calculation using the above method, which does not take into account the previous surface shift, will produce an error, especially at a low instrument oscillation amplitude.

Taking into account the previous shift, we assume that the treated part surface also has a shear stiffness k_τ in the direction of the formed working cone of deforming element (Dragobetskii et al. 2015, Ogorodnikov et al. 2004, Vasilevskyi 2013). Taking the above into account, let us consider the following situations.

Case II. Friction coefficient

$$\eta \le k_\tau ctg\alpha / k_n \tag{16.10}$$

The characteristic of the tangential interaction for this case is as follows:

$$F_{fr}(u,\dot{u}) = \begin{cases} \eta N & \dot{u} \ge 0 \\ \eta N - k_\tau(u_m - u)\cos\alpha & u_m - \frac{2S}{1+m} \le u \le u_m \quad \dot{u} \le 0 \\ -\eta(N - k_n(u_m - u))\sin\alpha & u_m - S \le u \le u_m - \frac{2S}{1+m} \quad \dot{u} \le 0 \\ 0 & u_m - S \le u \quad \dot{u} \le 0 \end{cases} \tag{16.11}$$

where $m = \frac{k_\tau}{k_n \eta} c\,\text{tg}\alpha$.

The total characteristic in the direction of the movement is similar to (16.9).

Figure 16.3a and b show the dependencies (16.4) and (16.11). Sections 16.1 and 16.2 show the characteristics of friction force (Figure 16.3b), corresponding to the load – there is a sliding of surfaces; in Section 16.3 – the elastic unloading with further negative elastic tension due to the friction; in Section 16.4 – unloading with slippage. The solid line in Figure 16.3c shows the total characteristic, and the dashed one – its components: $N(u,\dot{u})$, $F_{fr}(u,\dot{u})$.

If the amplitude of tool oscillations is $\xi \le S_1/2$, a purely elastic interaction takes place, which is established after the transition process (Section 16.5, Figure 16.3c). Here the material behaves as elastic–plastic with a rigidity coefficient:

$$k = k_n \sin^2\alpha + k_\tau \cos^2\alpha \tag{16.12}$$

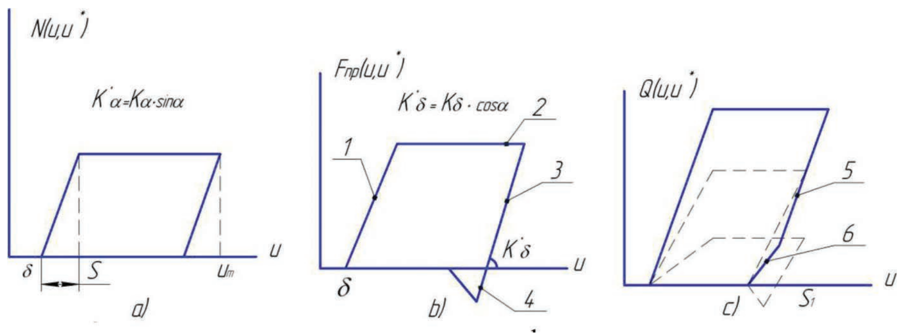

Figure 16.3 Load diagram at $\eta \le \frac{k_\tau}{k_n} c\,\mathrm{tg}\,\alpha$.

Note that according to (16.11):

$$S_1 = 2S/(1+m) \tag{16.13}$$

As shown in (16.12), (16.13), k_τ and η are important in calculating the total rigidity coefficient. For example, when $\alpha = 5^\circ$ $k \approx 0{,}0076k_n + 0{,}99k_\tau$.

Under these conditions, all conclusions are valid (Romashkyna 2009), according to which:

$$Q_y = Q - \xi \cdot k\left(\text{at}\,\xi \le S_1\right) \tag{16.14}$$

where Q_y, Q – stretching forces with ultrasound and without it, respectively.

At large amplitudes, nonlinear distortions begin, associated with the approach to the characteristic branch, marked by line 6 in Figure 16.3c. In this case, there are slippage and friction losses on the contact surfaces of the tool and the part.

Case III. If the friction coefficient is

$$\eta \ge k_\tau \cdot ctg \cdot \alpha / k_n \tag{16.15}$$

the characteristic of tangential interaction has the following form:

$$F_{fr}(u,\dot{u}) = \begin{cases} 0 & u \le \Delta \\ k_\tau(u-\Delta)\cos\alpha & u \le \Delta + S/m \quad \dot{u} \ge 0 \\ \eta \cdot N & \Delta + S/m \le u \le u_m \quad \dot{u} \ge 0 \\ \eta \cdot N(u,\dot{u}) & \dot{u} \le 0 \quad \dot{u} \ge 0 \end{cases}, \tag{16.16}$$

Figure 16.4b shows the characteristics (16.4) (16.16). Line 1 in Figure 16.4b shows tangent characteristics (16.16), elastic deformation takes place; 2 – slipping; 3 – unloading with slippage. The total characteristic is presented in Figure 16.4c. Here the elastic deformation zone is limited by line 4.

For the three cases at $\xi \ge S_1$, with the help of the impulse theorem, substituting in (17) the relevant characteristics of normal and tangential interactions, the correlation

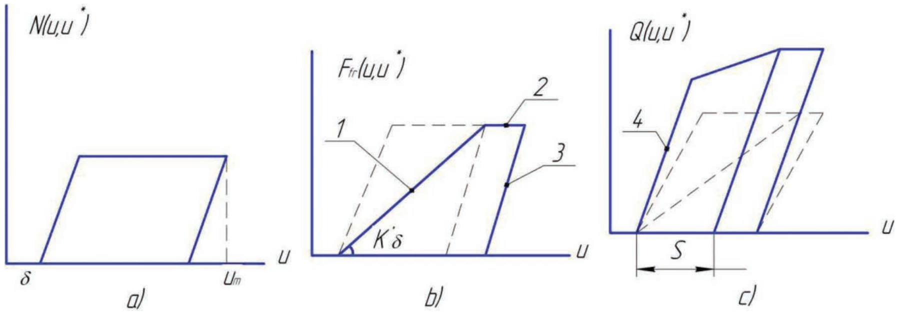

Figure 16.4 Load diagram at $\eta \geq \frac{k_\tau}{k_n} c\,\mathrm{tg}\,\alpha$.

that ties a constant statistical force with parameters of tool motion and the characteristics of the processed material can be obtained:

$$Q_y = \frac{1}{T} \int_{t_1}^{t_1+T} (N(u,\dot{u})\sin\alpha + F_{fr}(u,\dot{u})\cos\alpha)\,dt \tag{16.17}$$

To check received dependencies, experiments were conducted involving stretching out of steel 10 sleeves with the dimensions (mm): outer diameter – 30, hole diameter – 10, deforming element tension – 0.2. The sleeves were processed using carbide deforming elements with a 5° angle of inclination. Sulfofresol was used as a lubricant.

The stiffness of the linear section of the detail in the normal direction was determined using the method described in (Turych et al. 2018). For investigated details, it was $k_n = 5.92 \cdot 10^6$ MN/m.

Tangential stiffness was determined as follows. From the processed sleeve, microfloors were made and photographed. The photograph shows that the metal grains have a typical, pronounced texture, that is, grain elongation and inclination in the direction of stretching. The value of grain elongation was measured on several sections of microfloors, and then the average value X_0 was determined. Using the technique, the normal force and friction force were determined (Shao-Yi 2016). The value of the tangential stiffness was determined as the ratio of friction to X_0:

$$k_\tau = F_{fr} / X_0 \tag{16.18}$$

For the experiments, the value was 6.02×10^5 MN/m.

As the stretching was conducted with a maximum vibration amplitude of 15 mm, and the mean $S_1/2$ was 17 mm, the stretching force was determined by the dependence (14). The experimental and calculated values of the forces were well coincided, the difference amounted to no more than 15%.

The analysis provides a clear picture of the contact interaction between a tool and a product surfaces during stretching deformation using ultrasound and also makes it possible to calculate the stretching force, observed in different conditions of contact interaction.

16.5 CONCLUSIONS

The obtained theoretical dependences for calculating stretching forces, when processing with the use of ultrasound, show that the mechanism of influence of ultrasound on reduction of stretching forces is manifested in the accumulation of small plastic deformations, which increase between periods of fluctuations due to the total vibrational and translational motions of the tool and reduce friction forces by changing the kinematics of sliding.

It was established that the type of contact interaction between the tool with the detail has a decisive impact on how ultrasounds reduce stretching forces. With impulse interaction (with a break between contact of instrument and detail surfaces), stretching force is reduced to a minimum, tending toward zero, and in unceasing (without breaking of contact between surfaces) – by 60%–70% in comparison to stretching force without the use of ultrasound.

The construction of the deforming tool for deformation processing with the use of ultrasound was proposed.

REFERENCES

Dragobetskii, V., Shapoval, A., Mos'pan, D., Trotsko, O. & Lotous, V. 2015. Excavator bucket teeth strengthening using a plastic explosive deformation. *Metallurgical and Mining Industry* 4: 363–368.

Kozlov, L.G., Polishchuk, L.K., Piontkevych, O.V., Korinenko, M.P., Horbatiuk, R.M., Komada, P., Orazalieva, S. & Ussatova, O. 2019. Experimental research characteristics of counter balance valve for hydraulic drive control system of mobile machine. *Przeglad Elektrotechniczny* 95(4): 104–109.

Kumar, J. 2013. Ultrasonic machining-a comprehensive review. *Mach. Sci. and Technol.* 3: 325–379.

Landeta, J.F., Valdivielso, A.F., Lacalle, L.L., Girot F. & Pérez, J.P. 2015. Wear of Form Taps in Threading of Steel Cold Forged Parts. *Journal of Manufacturing Science and Engineering* 137(3): 1–11.

Mashkov, V., Smolarz, A., Lytvynenko, V. & Gromaszek, K. 2014. The problem of system fault-tolerance. *Informatyka, Automatyka, Pomiary w Gospodarce i Ochronie Środowiska* 4: 41–44.

Moriwaki, T. 2010. Development of 2DOF ultrasonic vibration cutting device for ultraprecision elliptical vibration cutting. *Key Engineering Materials* 447–448: 164–168.

Ogorodnikov, V.A., Dereven'ko, I.A. & Sivak, R.I. 2018. On the Influence of Curvature of the Trajectories of Deformation of a Volume of the Material by Pressing on Its Plasticity Under the Conditions of Complex Loading. *Materials Science* 54(3): 326–332.

Ogorodnikov, V.A., Savchinskij, I.G. & Nakhajchuk, O.V. 2004. Stressed-strained state during forming the internal slot section by mandrel reduction. *Tyazheloe Mashinostroenie* 12: 31–33.

Ogorodnikov, V.A., Zyska, T. & Sundetov, S. 2018. The physical model of motor vehicle destruction under shock loading for analysis of road traffic accident. *Proc. SPIE* 108086C: 1–5.

Polishchuk, L., Bilyy, O. & Kharchenko, Y. 2016. Prediction of the propagation of crack-like defects in profile elements of the boom of stack discharge conveyor. *Eastern-European Journal of Enterprise Technologies* 6(1): 44–52.

Polishchuk, L., Gromaszek, K., Kozlov, L.G. & Piontkevych, O.V. 2019. Study of the dynamic stability of the belt conveyor adaptive drive. *Przeglad Elektrotechniczny* 95(4): 98–103.

Polishchuk, L., Kozlov, L.G., Piontkevych, O.V., Gromaszek, K. & Mussabekova, A. 2018. Study of the dynamic stability of the conveyor belt adaptive drive. *Proc. SPIE 1080862*: 1791–1800.

Rimkeviciene, J., Ostasevicius, V., Jurenas, V. & Gaidys, R. 2009. Experiments and simulations of ultrasonically assisted turning tool. *Mechanika (Lietuva)* 75(1): 42–46.

Romashkyna, O.V. 2009. Yssledovanye vlyianyia parametrov ultrazvukovoi obrabotkyna formyrovanye ostatochnikh napriazhenyi pry narezanyy naruzhnikh rezb maloho dyametra. *VestnykSamHTU. Ser. Tekhnycheskyenauky* 2: 113–119.

Shao-Yi, H., Yu-Tuan, C. & Guan-Fan, L. 2016. Analysis of Sheet Metal Tapping Screw Fabrication Using a Finite Element Method. *MPDI Appl. Sci*. 6: 1–15.

Titov, A.V., Mykhalevych, V.M., Popiel, P. & Mussabekov, K. 2017. Statement and solution of new problems of deformability theory. *Proc. SPIE 108085E*: 1611–1617.

Turych, V.V. & Rutkevych, V.S. 2016. Kontaktna vzaiemodiia instrumenta z detalliu v protsesi deformuiuchoho protiahuvannia z ultrazvukom. *Promyslova hidravlika i pnevmatyka* 4(54): 71–76.

Turych, V.V., Rutkevych, V.S., Goncharuk, N. & Ogorodnichuk, G. 2018. Investigation of the process of smoothing with ultrasound. *Eastern–European Journal of Enterprise Technologies. Engineering technological systems* 3(93): 22–33.

Turych, V.V., Weselowskaya, N., Rutkevych, V. & Shargorodskiy, S. 2017. Investigation of the process of thread extrusion using the ultrasound. *Eastern–European Journal of Enterprise Technologies. Engineering technological systems* 6(90): 60–68.

Tymchyk, S.V., Skytsiouk, V.I., Klotchko, T.R., Ławicki, T. & Denisova, N. 2018. Distortion of geometric elements in the transition from the imaginary to the real coordinate system of technological equipment. *Proc. SPIE* 108085C: 1595–1604.

Vasilevskyi, O.M. 2013. Advanced mathematical model of measuring the starting torque motors. *Technical Electrodynamics* 6: 76–81.